# Variable magnetic interactions in an organic radical system of (*m*-*N*-methylpyridinium α-nitronyl nitroxide)·$X^-$: A possible *kagomé* antiferromagnet

Kunio Awaga, Tsunehisa Okuno, Akira Yamaguchi, and Morikuni Hasegawa
*Department of Pure and Applied Sciences, The University of Tokyo, Komaba, Meguro, Tokyo 153, Japan*

Tamotsu Inabe
*Department of Chemistry, Faculty of Science, Hokkaido University, Sapporo 060, Japan*

Yusei Maruyama
*Institute for Molecular Science, Myodaiji, Okazaki 444, Japan*

Nobuo Wada
*Institute of Physics, The University of Tokyo, Komaba, Meguro, Tokyo 153, Japan*
(Received 16 August 1993)

In this paper we study an organic system of geometrical spin frustration. *m*-*N*-methylpyridinium α-nitronyl nitroxide (*m*-MPYNN$^+$) is a spin-$\frac{1}{2}$ organic radical. The simple salt, *m*-MPYNN$^+$·$ClO_4^-$·$\frac{1}{3}$ (acetone), crystallizes in a trigonal $P3c1$ space group, where the *m*-MPYNN$^+$ molecules exist as a dimer and the dimer units form a two-dimensional (2D) triangular lattice. One-third of the $ClO_4^-$ ions are in the organic layer, joining the *m*-MPYNN$^+$ molecules, and the remainder is between the layers, compensating the excess of positive charge in the organic layers. The single-crystal EPR measurements clearly indicate a 2D Heisenberg character of the magnetic system in it. *m*-MPYNN$^+$ makes a crystalline solid-solution system, *m*-MPYNN$^+$·$(ClO_4^-)_x$·$I^-_{1-x}$·$\frac{1}{3}$ (acetone) ($0 \le x \le 1$), which also belongs to the trigonal system. Both the *a* and *c* axes are slightly lengthened with increasing the ratio of the $ClO_4^-$ ion, *x*, in the solid solution: The unit-cell volume is increased by 3.2% when *x* runs from 0 to 1. The temperature dependence of the magnetic susceptibilities of the solid solutions can be well interpreted in terms of a strong ferromagnetic intradimer interaction $J_1$ forming a triplet state and a weak antiferromagnetic interdimer interaction $J_2$ which is expected to give rise to spin frustration among the triplet spin species on each side of the triangles. It is found that $J_2$ quickly weakens with an increase in *x*, while $J_1$ shows little dependence. There is a possibility that this organic system can be characterized as a spin-1 *kagomé* antiferromagnet at very low temperatures.

## I. INTRODUCTION

Geometrical frustration in antiferromagnetic systems with triangular coordination symmetry is of much interest to recent physics. In such a triangle, two nearest neighbors to a given spin are themselves nearest neighbors and antiferromagnetic couplings among them cannot be completely satisfied. The frustration prevents long-range magnetic order from being established and allows novel kinds of low-temperature magnetic states to develop.[1-3] Ground states are governed by secondary effects such as next-nearest-neighbor interactions,[4] single-ion magnetic anisotropy, or possibly by quantum fluctuations,[5] and might be expected to possess highly material-dependent characteristics.

From the viewpoint of materials, the frustrated systems which have been experimentally studied so far, are limited to be inorganic.[6] Recently we have found an antiferromagnetic triangular lattice in the crystal of an organic cation radical, *m*-*N*-methylpyridinium α-nitronyl nitroxide (*m*-MPYNN$^+$). We have already reported[7] a preliminary work on the magnetostructural correlation in a complex salt, *m*-MPYNN$^+$·$(BF_4^-)_{0.72}$·$I^-_{0.28}$ [·0.17 ($H_2O$)] [there is an ambiguity in 0.17 ($H_2O$)]. The detailed structure analysis of this crystal was continued, but refinement of the structure was unsuccessful, presumably due to the fact that it includes disorder of the anions and the crystal solvent in both occupancy and orientation. In this paper we describe in detail the structure of a simple salt, *m*-MPYNN$^+$·$ClO_4^-$·$\frac{1}{3}$ (acetone), which has been successfully refined. In addition, structural and magnetic properties of the *m*-MPYNN$^+$·$(ClO_4^-)_x$·$I^-_{1-x}$·$\frac{1}{3}$ (acetone) ($0 \le x \le 1$) system are reported. There is a possibility that this magnetic system can be characterized as a spin-1 *kagomé* antiferromagnet at very low temperatures. The Heisenberg *kagomé* antiferromagnet is one of the most interesting of the frustrated systems.[8] The classical *kagomé* antiferromagnet exhibits a rich, nontrivial ground-state degeneracy, permitting a noncoplanar 120° spin orientation, or a what is called paper Origami structure, in addition to a coplanar configuration.[9]

## II. EXPERIMENT

Crystals of the *m*-MPYNN$^+$·$(ClO_4^-)_x$·$I^-_{1-x}$·$\frac{1}{3}$ (acetone) ($0 \le x \le 1$) system were prepared by the same

 

TABLE I. Results of the elemental analyses for $m$-MPYNN$^+\cdot(ClO_4^-)_x\cdot I^-_{1-x}\cdot\frac{1}{3}$ (acetone).

| $x$ | | C | H | N | Cl | I |
|---|---|---|---|---|---|---|
| 0.64 | Obs | 44.18 | 5.41 | 10.71 | 5.68 | 11.73 |
| | Calc | 44.48 | 5.60 | 11.11 | 5.98 | 12.14 |
| 0.90[a] | Obs | 45.36 | 5.78 | 11.01 | | |
| | Calc | 45.33 | 5.70 | 11.34 | | |
| 1.00 | Obs | 45.55 | 5.52 | 11.46 | 9.63 | |
| | Calc | 45.68 | 5.75 | 11.41 | 9.63 | |

[a]This was determined only from the observed mass percentage of C, H, and N.

procedures described previously.[7,10,11] They grew from acetone solutions, including one acetone molecule per three $m$-MPYNN$^+\cdot X^-$ units. The ratio of $ClO_4^-$ to $I^-$ was determined from the results of elemental analyses shown in Table I.

Crystallographic examination of the $m$-MPYNN$^+\cdot(ClO_4^-)_x\cdot I^-_{1-x}\cdot\frac{1}{3}$ (acetone) system was performed on a Rigaku AFC-5 automatic four-circle diffractometer with graphite-monochromatized Mo $K_\alpha$ radiation. Unit-cell dimensions of the solid solution system were obtained by least-squares refinement using 20 reflections for which $20°<2\theta<25°$. A detailed structure analysis for $m$-MPYNN$^+\cdot ClO_4^-\cdot\frac{1}{3}$ (acetone) was carried out on an approximately $0.5\times0.4\times0.3$ mm$^3$ crystal. A total of 4658 reflections were collected in the range of $4°<2\theta<50°$, monitoring three check reflections during every 100 reflections. No loss of intensity was shown during the course of data collection. 2525 reflections with $F>3\sigma(F)$ were used for structure refinement. The crystal structure was solved by direct methods (SAPI85) and the positions of the hydrogen atoms were obtained from calculation. A block-diagonal least-squares technique (UNICS III) was employed for the structure refinement in which the nonhydrogen atoms in the $m$-MPYNN$^+$ molecule were treated with anisotropic thermal parameters and the hydrogen atoms were refined with isotropic parameters. Final values of $R=0.097$ and $R_w=0.083$ were obtained.

The static magnetic susceptibility was measured in a field of 1 T by using a Faraday balance. The details of the apparatus were described previously.[12] $X$-band electron paramagnetic resonance (EPR) spectra were measured with a JES-RE2X spectrometer.

Crystals of the simple iodide salt, $m$-MPYNN$^+\cdot I^-$ [$\cdot\frac{1}{3}$ (acetone)] [there is an ambiguity in $\frac{1}{3}$(acetone)], are not stable. In the air they immediately turn into mosaic by evaporation of the crystal solvent. Unit-cell and magnetic measurements for $m$-MPYNN$^+\cdot I^-$ were, therefore, done on samples coated by an Araldite Rapid adhesive. The other crystals including $ClO_4^-$ are stable.

## III. RESULTS AND DISCUSSION

### A. Structure

X-ray crystal analysis has been carried out on the stable simple salt, $m$-MPYNN$^+\cdot ClO_4^-\cdot\frac{1}{3}$(acetone). Unit-cell dimensions are given in Table II. Table III shows the fractional coordinates and equivalent isotropic thermal parameters for the $m$-MPYNN$^+$ molecules. Table IV shows the fractional coordinates, equivalent isotropic thermal parameters, and occupancy for the $ClO_4^-$ ions and the acetone molecule. The structure crystallized into a trigonal $P3c1$ space group with $Z=12$. In the previous report concerning $m$-MPYNN$^+\cdot(BF_4^-)_{0.72}\cdot I^-_{0.28}$ [$\cdot0.17(H_2O)$] [there is an ambiguity in $0.17(H_2O)$], we reported the space group to be $P\bar{3}c1$. However, this now appears to be incorrect. We speculate that the disorder in occupancy of $BF_4^-$ and $I^-$ gave us an average structure in appearance, leading to the incorrect higher symmetry.

The $m$-MPYNN$^+$ molecules in the crystal are manifested as dimers in which the two molecules are related by a pseudoinversion symmetry, and the dimer units form a two-dimensional (2D) triangular lattice parallel to the $ab$ plane. Figure 1(a) shows a projection of the organic layer of $m$-MPYNN$^+$ onto the $ab$ plane. The radical dimer is located on each side of the triangles. In other words, the $m$-MPYNN$^+$ radical molecules form a bond-

TABLE II. Lattice constants and magnetic parameters for the $m$-MPYNN$^+\cdot(ClO_4^-)_x\cdot I^-_{1-x}\cdot\frac{1}{3}$ (acetone) system.

| $x$ | 0.00 | 0.64 | 0.90 | 1.00 | $m$-MPYNN$^+\cdot(BF_4^-)_{0.72}\cdot I^-_{0.28}$[a] |
|---|---|---|---|---|---|
| $a$ (Å) | 15.876(5) | 15.980(4) | 15.995(1) | 16.023(5) | 15.938(1) |
| $c$ (Å) | 23.583(6) | 23.752(4) | 23.891(2) | 23.893(4) | 23.615(1) |
| $V$ (Å$^3$) | 5147(3) | 5253(2) | 5284.5(5) | 5312(2) | 5194.9(3) |
| $C$ (emu K mol$^{-1}$) | | 0.378 | 0.376 | 0.379 | 0.377[b] |
| $J_1/k_B$ (K) | 10.2 | 10.4 | 10.4 | 10.5 | 11.3[b] |
| $J_2/k_B$ (K) | −1.60 | −0.81 | −0.56 | −0.19 | −1.20[b] |

[a]Reference 7.

[b]The magnetic data in Ref. 7 were reinterpreted using Eq. (3) in this work.

alternated hexagonal lattice, as is schematically shown in Fig. 1(b). Figure 2 shows a side view of the trigonal lattice, where nine units of the *m*-MPYNN$^+$ dimers on the surface of the hexagonal prism are drawn. The unit cell includes two organic layers at the height of $z=0$ and $z=\frac{1}{2}$, between which there is a big separation.

The counter parts (the $ClO_4^-$ ions and the acetone molecules) are nearly located on the $z=0$, $\frac{1}{4}$, $\frac{1}{2}$, and $\frac{3}{4}$ planes in the unit cell with orientational disorder. Figure 3(a) schematically shows their positions on the $z=0$ plane which is in the organic radical layer. Only the $ClO_4^-$ ions (open circles) appear at the centers of the triangles, each of which is surrounded by the three *m*-MPYNN$^+$ dimer units. In this organic layer, the ratio of *m*-MPYNN$^+$:$ClO_4^-$ is 3:1. Figure 3(b) shows the counterpart positions on the $z=\frac{1}{4}$ plane which is between the organic layers. The $ClO_4^-$ ions (open circles) are located on the sides of the triangles and the acetone molecules (closed circles) are located at the centers of them. The $z=\frac{1}{2}$ and $\frac{3}{4}$ planes are related to the $z=0$ and $\frac{1}{4}$ planes, respectively, by a rotation of 60° around the *c* axis. This means that there is a channel of the counter parts along the *c* axis in the center of the triangle, where $ClO_4^-$ and acetone appear alternately. It is quite interesting that one-third of the $ClO_4^-$ ions are in the organic layer, joining the *m*-MPYNN$^+$ molecules, and the remains are between the layers, compensating the excess of positive charge in the organic layers.

TABLE III. Fractional coordinates (×1000) and isotropic thermal parameters for the *m*-MPYNN$^+$ molecules.

| Atom | *x* | *y* | *z* | $B_{eq}$ |
|---|---|---|---|---|
| O(1) | 1524(5) | 3083(5) | −127(3) | 3.4(0.3) |
| O(2) | −1065(5) | 3229(5) | −897(3) | 3.5(0.3) |
| N(3) | 881(7) | 3000(6) | −479(3) | 3.6(0.3) |
| N(4) | −358(7) | 3088(7) | −837(5) | 5.0(0.4) |
| C(5) | 241(6) | 3333(7) | −375(4) | 3.0(0.3) |
| C(6) | 638(9) | 2420(9) | −1000(4) | 4.6(0.5) |
| C(7) | −16(11) | 2668(10) | −1282(4) | 5.0(0.6) |
| C(8) | 1544(9) | 2578(11) | −1273(5) | 5.1(0.6) |
| C(9) | 113(15) | 1335(11) | −777(6) | 7.8(0.9) |
| C(10) | 602(18) | 3568(12) | −1706(7) | 10.7(1.2) |
| C(11) | −881(13) | 1869(12) | −1579(8) | 8.6(0.9) |
| C(12) | 165(9) | 3752(7) | 128(5) | 3.9(0.4) |
| C(13) | 973(8) | 4255(7) | 469(4) | 3.2(0.4) |
| N(14) | 895(6) | 4680(6) | 930(3) | 3.5(0.3) |
| C(15) | 129(9) | 4631(8) | 1107(4) | 3.9(0.5) |
| C(16) | −717(9) | 4176(8) | 775(4) | 4.0(0.4) |
| C(17) | −710(8) | 3703(7) | 287(5) | 3.6(0.4) |
| C(18) | 1797(9) | 5254(9) | 1250(6) | 5.5(0.5) |
| O(19) | 3116(8) | 1606(7) | 126(4) | 6.6(0.5) |
| O(20) | 3263(8) | 4305(7) | 865(4) | 6.5(0.5) |
| N(21) | 3015(7) | 2149(6) | 444(3) | 3.5(0.3) |
| N(22) | 3075(5) | 3431(5) | 809(2) | 2.2(0.2) |
| C(23) | 3295(7) | 3067(8) | 372(4) | 3.5(0.4) |
| C(24) | 2403(10) | 1780(8) | 973(5) | 4.6(0.5) |
| C(25) | 2709(8) | 2720(8) | 1301(4) | 3.6(0.4) |
| C(26) | 1366(9) | 1306(8) | 781(6) | 4.9(0.5) |
| C(27) | 2558(16) | 1013(14) | 1251(6) | 9.3(1.0) |
| C(28) | 3492(15) | 2975(11) | 1682(6) | 8.1(0.9) |
| C(29) | 1950(15) | 2813(12) | 1601(6) | 8.6(0.9) |
| C(30) | 3803(7) | 3631(7) | −144(3) | 2.3(0.3) |
| C(31) | 4315(8) | 3332(8) | −447(4) | 3.1(0.4) |
| N(32) | 4735(6) | 3757(6) | −952(4) | 3.4(0.3) |
| C(33) | 3664(8) | 4564(8) | −1112(5) | 4.1(0.4) |
| C(34) | 4136(9) | 4844(8) | −821(5) | 3.9(0.4) |
| C(35) | 3748(8) | 4405(8) | −310(5) | 3.9(0.4) |
| C(36) | 5274(8) | 3428(9) | −1296(4) | 3.8(0.5) |

As is discussed in Ref. 7, there is a very short intermolecular contact between the NO group and the pyridinium ring in the intradimer molecular arrangement, which would be caused by the Coulombic attraction force between the positive charge on the pyridinium ring and the negative charge polarized on the O atom in the NO group. In the nitronyl nitroxide radical molecule, the magnetic orbital accommodating the unpaired electron is known to be localized on the two NO groups.[13] The intermolecular contact between the NO group and the pyridinium ring in the adjacent molecule, therefore, means an intermolecular interaction between the magnetic orbital and the nonmagnetic orbitals. The nonmagnetic orbits are naturally orthogonal to its magnetic orbital in the adjacent molecule. A ferromagnetic coupling can be predicted in the dimer through the [NO group]-[pyridinium ring]-[NO group] superexchange pathway. In the interdimer arrangement, on the other hand, there is a weak contact between the NO groups. Such an NO $\cdots$ NO contact means a direct intermolecular interaction between the magnetic orbitals, which always leads to an antiferromagnetic coupling.

*m*-MPYNN$^+$ makes a solid solution system, *m*-MPYNN$^+\cdot(ClO_4^-)_x\cdot I^-_{1-x}\cdot\frac{1}{3}$ (acetone). We compare the unit-cell dimensions of the $x=0.00$, 0.64, 0.90, and 1.00 solid solutions in Table II, together with those of *m*-MPYNN$^+\cdot(BF_4^-)_{0.72}\cdot I^-_{0.28}$.[7] All the crystals belong to the trigonal system. Both lattice constants *a* and *c*, are slightly increased, with increasing the ratio of the $ClO_4^-$ ion whose size is larger than that of the $I^-$ ion. This is quite natural to the fact that the anions occupy both the open spaces in the 2D lattice of the *m*-MPYNN$^+$ molecules and the gap between the 2D layers. The unit-cell volume is increased by 3.2%, when *x* changes from 0 to 1.

### B. Magnetic properties

*X*-band EPR measurements were performed on the *m*-MPYNN$^+\cdot ClO_4^-\cdot\frac{1}{3}$ (acetone) single crystal at room temperature in order to confirm a 2D character of the magnetic system in it. The line shape was close to a Lorentzian shape, while it depended slightly on direction of the external field. Whereas a 1D magnetic system has an EPR line showing a large deviation from a Lorentzian shape, the deviation of a 2D system is very small.[14]

Figure 4 shows *g*-value anisotropy in the *ac* (open circles) and *ab* (closed circles) planes. $\theta$ is the angle between the external field and the *c* axis in the *ac* plane and that between the field and the *a* axis in the *ab* plane, respectively. The *g* value shows no anisotropy in the *ab* plane, while it depends on $\theta$ in the *ac* plane. The *g* value of a trigonal system should be written as

$$g^2=g_{\parallel}^2\sin^2\theta+g_{\perp}^2\cos^2\theta\ , \tag{1}$$

TABLE IV. Fractional coordinates ( $\times 1000$), isotropic thermal parameters, and occupancy for the $ClO_4^-$ ions and the acetone molecule.

| Atom | $x$ | $y$ | $z$ | $B_{eq}$ | Occupancy |
|---|---|---|---|---|---|
| Cl(37) | 380(0) | 17(0) | 247(0) | 6.4(0.1) | 1.0 |
| O(38) | 417(2) | 119(2) | 230(1) | 13.5(0.7) | 0.5 |
| O(39) | 310(1) | −39(1) | 203(1) | 6.3(0.3) | 0.5 |
| O(40) | 340(1) | 10(1) | 302(0) | 5.3(0.3) | 0.5 |
| O(41) | 463(1) | 9(1) | 250(1) | 5.9(0.3) | 0.5 |
| O(42) | 324(4) | −75(4) | 260(2) | 11.8(1.4) | 0.5 |
| O(43) | 365(2) | 67(2) | 286(1) | 4.0(0.5) | 0.5 |
| O(44) | 431(2) | −52(2) | 255(1) | 5.5(0.7) | 0.5 |
| O(45) | 444(4) | 101(4) | 209(2) | 10.9(1.3) | 0.5 |
| Cl(46) | 333(0) | 667(0) | −31(0) | 5.1(0.1) | 0.33 |
| O(47) | 297(0) | 686(0) | 18(1) | 6.9(0.7) | 0.33 |
| O(48) | 307(1) | 736(1) | −47(1) | 3.9(0.3) | 0.5 |
| O(49) | 309(1) | 728(1) | −72(1) | 4.6(0.3) | 0.5 |
| Cl(50) | 667(0) | 333(0) | 31(0) | 4.8(0.1) | 0.33 |
| O(51) | 667(0) | 333(0) | −27(1) | 13.5(0.9) | 0.33 |
| O(52) | 692(1) | 266(1) | 41(0) | 9.5(0.3) | 1.0 |
| Cl(53) | 0(0) | 0(0) | 249(0) | 5.2(0.1) | 0.33 |
| O(54) | 0(0) | 0(0) | 192(1) | 11.0(0.7) | 0.33 |
| O(55) | 62(2) | 104(2) | 244(1) | 11.1(0.8) | 0.5 |
| O(56) | 58(3) | 83(2) | 279(1) | 16.6(1.4) | 0.5 |
| O(57) | 665(0) | 332(0) | 285(1) | 10.3(0.6) | 0.33 |
| C(58) | 622(0) | 319(0) | 225(2) | 13.4(2.4) | 0.33 |
| C(59) | 585(3) | 289(4) | 198(2) | 6.5(1.0) | 0.33 |
| C(60) | 572(3) | 340(4) | 214(2) | 6.7(1.1) | 0.33 |
| O(61) | 333(0) | 667(0) | −293(1) | 6.0(0.4) | 0.33 |
| C(62) | 333(0) | 667(0) | −241(1) | 2.9(0.3) | 0.33 |
| C(63) | 250(4) | 615(4) | −198(2) | 7.3(1.1) | 0.33 |
| C(64) | 253(4) | 558(4) | −226(2) | 7.0(1.1) | 0.33 |

where $\theta$ is the angle between the field and the $c$ axis, and $g_{\parallel}$ and $g_{\perp}$ are two principal values, parallel and perpendicular to the $c$ axis, respectively. One can obtain a good fit using Eq. (1) with $g_{\parallel}=2.00603$ and $g_{\perp}=2.00579$, as is shown in Fig. 4 by the solid curves. The average $g$ value is calculated to be $\bar{g}=2.0059$. The $g$-value anisotropy in $m$-MPYNN$^+\cdot ClO_4^-\cdot\frac{1}{3}$ (acetone) is shown to be small, as is usual with most of the organic radicals.

Figure 5 shows the angular dependence of the peak-to-peak linewidth in the $ac$ (open circles) and $ab$ (closed circles) planes. The definition of $\theta$ is same as that in Fig. 4. When the field is in the $ab$ plane, the linewidth shows no dependence on the field direction, but when the field is in the $ac$ plane, it makes minimums at the magic angles. The angular dependence can be well fitted by the theoretical equation for a 2D magnetic system;[14]

$$\Delta H_{pp}=A(3\cos^2\theta-1)^2+B\ , \tag{2}$$

where $\theta$ is the angle between the field and the $c$ axis. The solid curves in Fig. 5 show the best fit, obtained with $A=0.094$ mT and $B=0.259$ mT. From the EPR measurements, it is concluded that the magnetic system is characterized as 2D Heisenberg spins. The magnetic interaction between the 2D layers is so weak that the high-temperature magnetic properties would be governed by two parameters, the intradimer interaction $J_1$ and the in-plane interdimer interaction $J_2$, shown in Fig. 1(b).

Temperature $T$ dependence of the paramagnetic susceptibilities $\chi_p$ of the $m$-MPYNN$^+\cdot(ClO_4^-)_x\cdot I^-_{1-x}\cdot\frac{1}{3}$ (acetone) system are shown in Fig. 6, where $\chi_pT$ is plotted as a function of $T$. The plots for $m$-MPYNN$^+\cdot I^-$ ($x=0$) are drawn, assuming the Curie constant to be the theoretical value of 0.376 emu K mol$^{-1}$ (with $g=2.006$), because we could not accurately weigh the sample coated by the adhesive. The four curves in Fig. 6 show rather similar temperature dependence: $\chi_pT$ increases as the temperature is decreased from room temperature down to $\sim 10$ K, indicating a ferromagnetic interaction. The intradimer magnetic coupling $J_1$ should be ferromagnetic. After passing through a maximum near 10 K, $\chi_pT$ shows a quick decrease which suggests that the interdimer magnetic interaction $J_2$ is antiferromagnetic. The observed behaviors are quite consistent with the intradimer and interdimer molecular arrangements. It is expected that the in-plane antiferromagnetic $J_2$ gives rise to spin frustration among the triplet spins formed by $J_1$. When the four curves in Fig. 6 are compared, the increase in $x$ leads to the increase in maximum value of $\chi_pT$ and to the decrease in temperature at the maximum $\chi_pT$. The observed temperature dependence can be well interpreted in terms of the ferromagnetic $J_1$ and the antiferromagnetic $J_2$, using

$$\chi_p=\frac{4C}{T[3+\exp(-2J_1/k_BT)]-4J_2/k_B}\ , \tag{3}$$

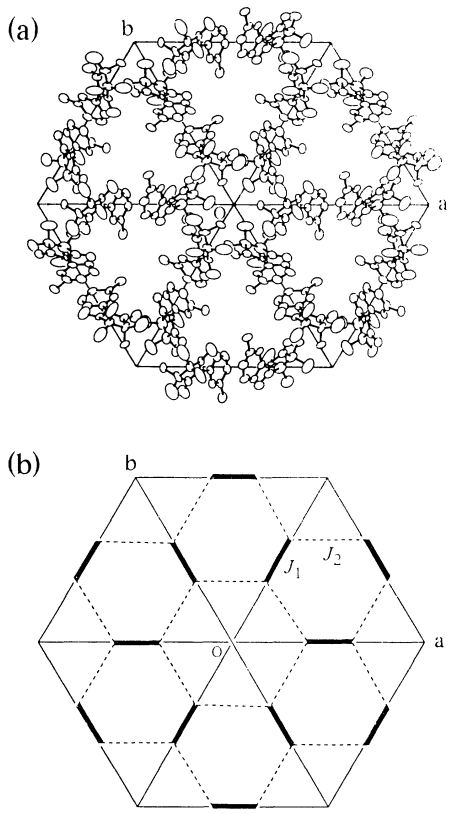


FIG. 1. (a) Organic 2D layer of *m*-MPYNN$^+$ projected onto the *ab* plane. (b) Bond-alternated hexagonal lattice. $J_1$ and $J_2$ are in-plane intradimer and interdimer magnetic interactions, respectively.

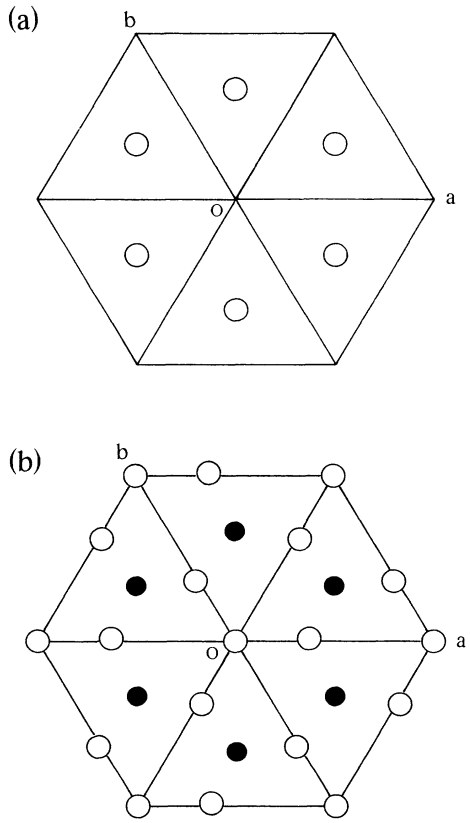


FIG. 3. Positions of the $ClO_4^-$ ions (open circles) and the acetone molecules (closed circles), on the $z=0$ plane (a) and the $z=\frac{1}{4}$ plane (b).

where $C$ is the Curie constant and $k_B$ is the Boltzmann constant. This equation was derived from the molecular-field approximation, as is shown in the Appendix. The solid curves in Fig. 6 are the theoretical best fit to the data, obtained with the parameters listed in Table II. When $x$ is close to 1, $|J_1/J_2| \gg 1$ is a good approximation. In this case, the magnetic system in this organic material could be characterized as a spin-1 *kagomé* antiferromagnet in the temperature range below $|J_2|/k_B$ K.

The two parameters $J_1$ and $J_2$ defined in the 2D plane, depend only on the size of the triangle. Figure 7 shows the dependence of $J_1$ (open circles) and $J_2$ (closed circles)

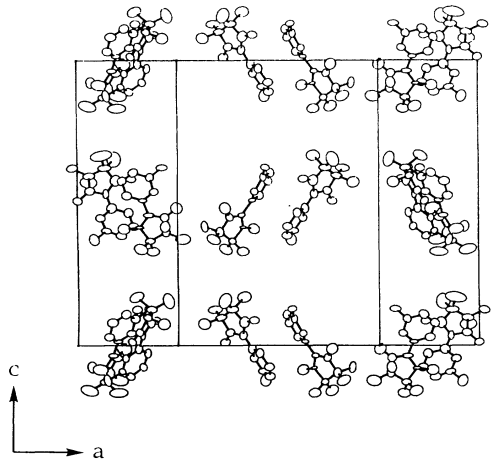


FIG. 2. Side view of the organic 2D layers. Nine *m*-MPYNN$^+$ dimers on the surface of the hexagonal prism are drawn.

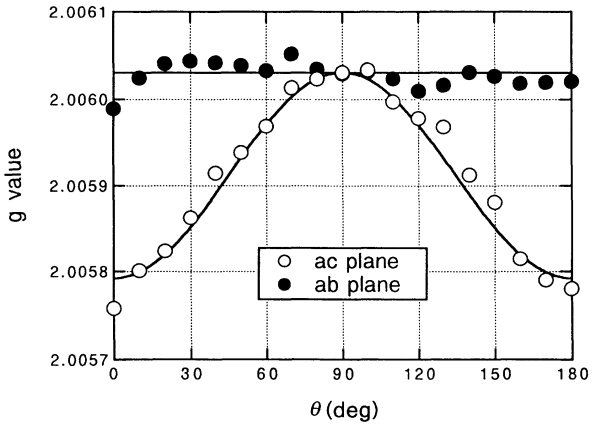


FIG. 4. Anisotropy of the EPR $g$ value in the *m*-MPYNN$^+$·$ClO_4^-$·$\frac{1}{3}$ (acetone) single crystal, in the *ac* (open circles) and *ab* (closed circles) planes. $\theta$ is the angle between the field and the *c* axis in the *ac* plane, and that between the field and the *a* axis in the *ab* plane, respectively. The theoretical curves are Eq. (1) of the text.

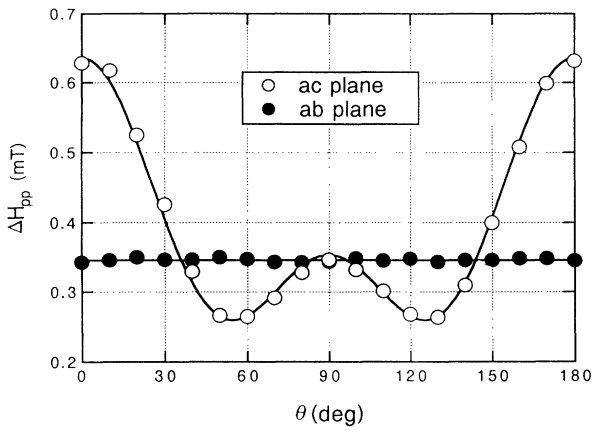


FIG. 5. Angular dependence of the peak-to-peak linewidth of the *m*-MPYNN$^+$·$ClO_4^-$·$\frac{1}{3}$ (acetone) single crystal, in the *ac* (open circles) and *ab* (closed circles) planes. $\theta$ is the angle between the field and the *c* axis in the *ac* plane, and that between the field and the *a* axis in the *ab* plane, respectively. The theoretical curves are Eq. (2) of the text.

on the length of the *a* axis in the *m*-MPYNN$^+$·$(ClO_4^-)_x$·$I^-_{1-x}$·$\frac{1}{3}$ (acetone) system, where $J_1$ and $J_2$ are normalized by the values of the $x=0$ crystal, respectively. The interdimer magnetic coupling $J_2$ quickly decreases down to $\sim\frac{1}{10}$ of the initial value during the change in $x$ from 0 to 1, while the intradimer magnetic coupling $J_1$ depends little on the lattice constant. This

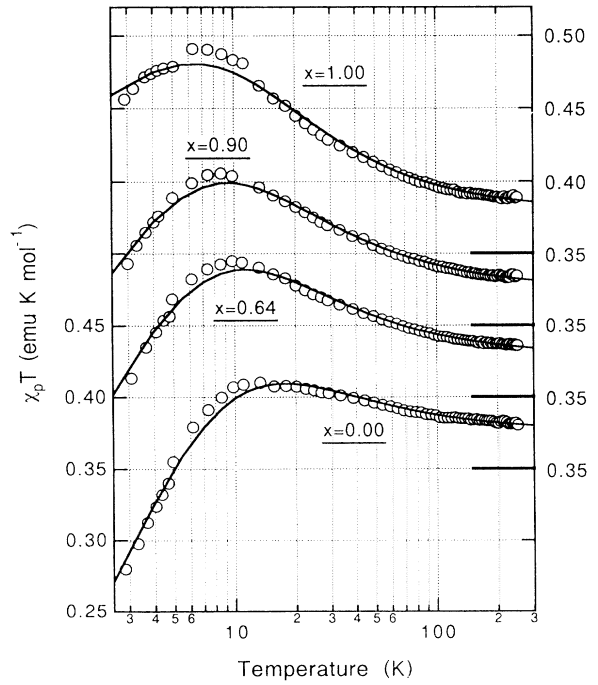


FIG. 6. Temperature dependence of the paramagnetic susceptibilities $\chi_p$ of *m*-MPYNN$^+$·$(ClO_4^-)_x$·$I^-_{1-x}$·$\frac{1}{3}$ (acetone) with $x=0.00$, 0.64, 0.90, and 1.00. The theoretical curves are Eq. (3) of the text. We assumed the Curie constant for *m*-MPYNN$^+$·$I^-$ to be the theoretical value of 0.376 emu K mol$^{-1}$.

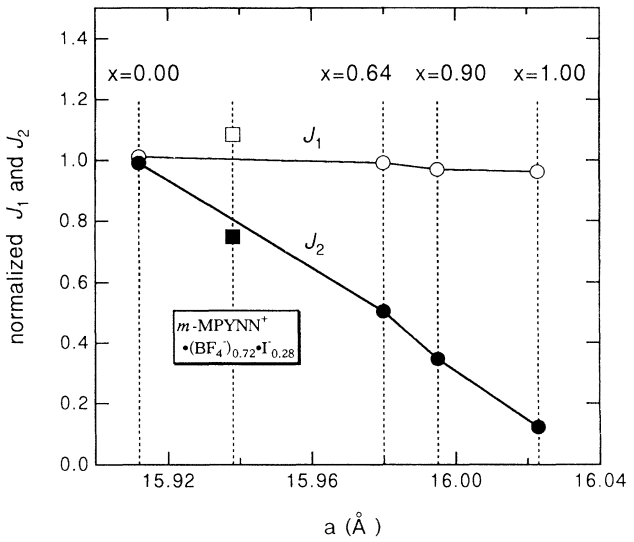


FIG. 7. Dependence of the intradimer ferromagnetic interaction $J_1$ (open circles) and the interdimer antiferromagnetic interaction $J_2$ (closed circles) of the *m*-MPYNN$^+$·$(ClO_4^-)_x$·$I^-_{1-x}$·$\frac{1}{3}$ (acetone) system, on the length of the *a* axis. $J_1$ and $J_2$ are normalized by the values of the $x=0$ crystal, respectively. The open and closed squares show normalized $J_1$ and $J_2$ of *m*-MPYNN$^+$·$(BF_4^-)_{0.72}$·$I^-_{0.28}$, respectively.

indicates that the intradimer molecular arrangement is very rigid and the spaces between the dimers increases with increasing the ratio of the larger $ClO_4^-$ ion. Figure 7 also shows $J_1$ (open square) and $J_2$ (closed square) for *m*-MPYNN$^+$·$(BF_4^-)_{0.72}$·$I^-_{0.28}$.[7] They are almost located on the lines between the plots for the *m*-MPYNN$^+$·$(ClO_4^-)_x$·$I^-_{1-x}$·$\frac{1}{3}$ (acetone) system, respectively. This suggests that the two parameters depend little on the chemical properties of the anion. It is unique of the *m*-MPYNN$^+$·$X^-$ system that the two magnetic parameters can be varied continuously. This is advantageous to revealing the physics of the antiferromagnetic *kagomé* lattice in detail.

## IV. SUMMARY

The $\alpha$-nitronyl nitroxide cation radical, *m*-MPYNN$^+$, shows quite a unique structure and magnetic properties. In a crystal of *m*-MPYNN$^+$·$(ClO_4^-)_x$·$I^-_{1-x}$·$\frac{1}{3}$ (acetone), the *m*-MPYNN$^+$ molecules form a 2D bond-alternated hexagonal lattice which includes a strong feromagnetic intradimer interaction $J_1$ and a weak antiferromagnetic interdimer interaction $J_2$. One-third of the $ClO_4^-$ ions are in the organic layer, and the remainder are between the layers. A 2D Heisenberg character is concluded from single-crystal EPR measurements. The high-temperature magnetic susceptibility can be well fitted by Eq. (3) derived from the molecular-field approximation. With an increase in ratio of the $ClO_4^-$ ion in the crystal, the triangular lattice shows a slight increase in dimensions, which gives little influence on $J_1$ but makes $J_2$ much weaker. We can expect geometrical frustration in this

system, caused by the antiferromagnetic interaction between the ferromagnetic dimers.


## ACKNOWLEDGMENTS

We thank M. Itakura and Professor S. Hikami of Tokyo University for useful discussions and comments. This work was supported by the Grant-in-aid for Scientific Research No. 05453051 and that of Priority Area "Molecular Magnetism" (Area No. 228/04242103) from the Ministry of Education, Science, and Culture, Japanese government. Support from New Energy and Industrial Technology Development Organization (NEDO) is also acknowledged.


## APPENDIX

In the following we will sketch the derivation of Eq. (3). According to the molecular-field approximation, the Hamiltonian for the magnetic dimer system shown in Fig. 1(b) can be written as

$$\hat{H}=-2J_1\mathbf{S}_1\cdot\mathbf{S}_2+g\mu_B H(S_1^z+S_2^z) -2zJ_2\langle S_1^z\rangle S_2^z-2zJ_2\langle S_2^z\rangle S_1^z \ , \tag{A1}$$

where $J_1$ and $J_2$ are the intradimer and interdimer magnetic coupling constants, respectively, and $z(=2)$ is the number of the nearest neighbors connected by $J_2$. In the paramagnetic state, one can set $\langle S_1^z\rangle=\langle S_2^z\rangle$. The eigenvalues and the eigenfunction are obtained as follows:

$$\begin{aligned} E_1&=-\frac{J_1}{2}-h, \quad \alpha(1)\alpha(2) \ , \\ E_2&=-\frac{J_1}{2}, \quad \frac{1}{\sqrt{2}}[\alpha(1)\beta(2)+\alpha(2)\beta(1)] \ , \\ E_3&=-\frac{J_1}{2}+h, \quad \beta(1)\beta(2) \ , \\ E_4&=\frac{3J_1}{2}, \quad \frac{1}{\sqrt{2}}[\alpha(1)\beta(2)-\alpha(2)\beta(1)] \ , \end{aligned} \tag{A2}$$

where

$$h=g\mu_B H+zJ_2\langle S^z\rangle \quad \text{with } \langle S^z\rangle=\langle S_1^z\rangle+\langle S_2^z\rangle \ . \tag{A3}$$

If we choose $E_2$ as zero point of the energy, the partition function and the free energy are given by

$$Z=\exp\left[-\frac{h}{k_BT}\right]+1+\exp\left[\frac{h}{k_BT}\right]+\exp\left[-\frac{2J_1}{k_BT}\right] \ , \tag{A4}$$

$$F/(N_A/2)=-k_BT\ln Z-\tfrac{1}{2}zJ_2\langle S^z\rangle^2 \ . \tag{A5}$$

$\langle S^z\rangle$ is determined so as to minimize the free energy. From $\partial F/\partial\langle S^z\rangle=0$ we obtain

$$\chi=\frac{(N_A/2)g\mu_B/\langle S^z\rangle}{H} =\frac{N_Ag^2\mu_B^2}{k_BT\{3+\exp(-2J_1/k_BT)\}-2zJ_2} \ . \tag{A6}$$


[1] P. Fazekas and P. W. Anderson, Philos. Mag. **30**, 423 (1974).
[2] X. G. Wen, F. Wilczek, and A. Zee, Phys. Rev. B **39**, 11 413 (1989).
[3] P. Chandra and P. Coleman, Phys. Rev. Lett. **66**, 100 (1991).
[4] R. Liebmann, *Statistical Mechanics of Periodic Frustrated Ising Systems* (Springer, Heidelberg, 1986).
[5] C. L. Henley, Phys. Rev. Lett. **62**, 2056 (1989).
[6] A. P. Ramirez, J. Appl. Phys. **70**, 5952 (1991), and references therein.
[7] K. Awaga, T. Inabe, T. Nakamura, M. Matsumoto, and Y. Maruyama, Chem. Phys. Lett. **195**, 21 (1992).
[8] I. Syozi, Prog. Theor. Phys. **6**, 306 (1951).
[9] I. Ritchey, P. Chandra, and P. Coleman, Phys. Rev. B **47**, 15 342 (1993); E. F. Shender, V. B. Cherepanov, P. C. Holdsworth, and A. J. Berlinsky, Phys. Rev. Lett. **70**, 3812 (1991).
[10] K. Awaga, T. Inabe, U. Nagashima, T. Nakamura, M. Matsumoto, Y. Kawabata, and Y. Maruyama, Chem. Lett. **1991**, 1777 (1991).
[11] A. Yamaguchi, K. Awaga, T. Inabe, T. Nakamura, M. Matsumoto, and Y. Maruyama, Chem. Lett. **1993**, 1443 (1993).
[12] K. Awaga and Y. Maruyama, Chem. Mater. **2**, 535 (1990).
[13] K. Awaga, T. Inabe, U. Nagashima, and Y. Maruyama, J. Chem. Soc. Chem. Commun. **1989**, 1617 (1989).
[14] P. M. Richards and M. B. Salamon, Phys. Rev. B **9**, 32 (1974).